

# Scandium-Enriched Nanoprecipitates in Aluminum Providing Enhanced Coarsening and Creep Resistance

Anthony De Luca, David C. Dunand, and David N. Seidman

## Abstract

The development of high temperature aluminum alloys able to operate up to 400 °C is crucial to replace steel and titanium and decrease the mass of vehicles in the automotive and aerospace industries. This review relates the past two decades of aluminum alloy engineering done at Northwestern University focusing on developing coherent L12 Al3M nanoprecipitates strengthened aluminum alloys that are coarsening and shear-resistant at high temperature. Starting with the Al-Sc binary system, each new generation of alloys has become more complex to improve the alloy's mechanical properties and coarsening resistance at high temperatures. The effects of rare-earth (Er, Y, Sm, Gd, Tb, Dy, Ho, Tm, Yb, Lu), transition metals (Zr, Ti, V, Nb, Ta), inoculants (Si, In, Sb, Sr, Ge, Zn) and solid solution (Mg, Li) elements onto the L12 Al3M precipitates is reviewed. The most recent alloys have optimized strength, coarsening resistance and lower prices, opening the doors to wider application uses.

## Keywords

Aluminum alloy • High-temperature alloy  
Precipitation strengthening

The automotive and aerospace industries have steadily reduced the environmental footprint of vehicles by making more efficient use of fuel. One way to achieve this goal is to decrease vehicle mass by an increased use of low-density aluminum alloys [1]. Those light-weight aluminum alloys

are limited, however, to temperatures below ~220 °C due to the dissolution or phase transformation of their strengthening nanoprecipitates. To utilize aluminum alloys for high-temperature applications in automotive and aerospace applications, one approach is to create coherent L12 nanoprecipitates, which strengthen the alloy by impeding dislocation motion and which are stable and coarsen slowly by diffusion at the operating temperature, using slow-diffusing elements. [2].

Several slow-diffusing transition elements (M) form nanometric diameter Al3M (L12) nanoprecipitates when precipitated from a supersaturated aluminum solid-solution [2], the most widely studied and least dense element being Sc. Trace amounts of Sc increase drastically the strength of aluminum alloys due to the formation of a high number density of nanometric Al3Sc (L12) nanoprecipitates coherent with the aluminum matrix [3–13]. For example, the microhardness of pure aluminum (200 MPa) can be increased fourfold by the addition of 0.18 at.% Sc [14, 15]. Due to the relatively high diffusivity of Sc, only a few hours at 300–350 °C are needed to achieve optimal precipitation of coherent Al3Sc (L12) nanoprecipitates and achieve peak microhardness. The alloy's long-term use cannot, however, exceed ~300 °C due to the coarsening of Al3Sc nanoprecipitates [14, 15].

Due to the small diffusivity of zirconium in aluminum [2], precipitation strengthening of Al–Zr alloys is extremely sluggish, generally needing more than 100 h of aging to achieve peak microhardness [16–21]. The metastable Al3Zr (L12) nanoprecipitates achieve relatively small number densities, so the strengthening effect is smaller than when using Sc, thus limiting usage of Al–Zr alloys. Al3Zr (L12) nanoprecipitates exhibit, however, a much higher coarsening resistance than Al3Sc (L12) nanoprecipitates. Alternatively, Er has a larger diffusivity than Sc [2, 22], and thus Al3Er (L12) nanoprecipitates nucleate and grow at low temperatures and Al–Er alloys suffer from an early loss of strength [23], preventing the use of Al–Er alloys for high-temperature applications. Due to the high lattice parameter mismatch

A. De Luca · D. C. Dunand (✉) · D. N. Seidman  
Department of Materials Science and Engineering, Northwestern University, 2220 Campus Drive, Evanston, IL 60208-3108, USA  
e-mail: dunand@northwestern.edu

D. C. Dunand · D. N. Seidman  
NanoAl LLC, Illinois Science + Technology Park, 8025 Lamon Ave, Suite 446, Skokie, IL 60077, USA

A. De Luca · D. N. Seidman  
Center for Atom-Probe Tomography, Northwestern University, 2220 Campus Drive, Evanston, IL 60208-3108, USA

between coherent  $\text{Al}_3\text{Er}$  ( $L1_2$ ) nanoprecipitates and the Al-matrix, those nanoprecipitates impart a high creep-resistance to Al–Er alloys.

The addition of Zr or Er to Al–Sc alloys respectively results in improvements in coarsening or creep resistance. In Al–Sc–Zr alloys, the coherent  $\text{Al}_3\text{Sc}$  ( $L1_2$ ) nanoprecipitates, which form during the early stages of aging serve as heterogeneous sites for precipitation of Zr, resulting in the formation of coherent core-shell  $\text{Al}_3(\text{Sc,Zr})$  ( $L1_2$ ) nanoprecipitates, with the core enriched in Sc and the shell enriched in Zr [9, 24–28]. Due to the formation of this Zr-rich shell with a small diffusivity, the precipitate coarsening rate is significantly reduced. Al–Sc–Er alloys behave similarly [29, 30]: Er atoms form *nuclei* onto which the Sc atoms precipitate, forming an Er-rich core surrounded by a Sc-rich shell. In this case, the Sc-shell prevents fast coarsening of coherent  $\text{Al}_3(\text{Sc,Er})$  ( $L1_2$ ) nanoprecipitates at elevated temperatures, just like Zr slows coarsening of coherent  $\text{Al}_3(\text{Zr,Sc})$  nanoprecipitates. The high number density of  $\text{Al}_3\text{Er}$  *nuclei* is maintained during aging, permitting the attainment of higher volume fractions and thereby increasing slightly the strength of the alloy at peak microhardness. Most importantly, the Er-rich core increases the lattice parameter mismatch of the nanoprecipitates with the Al-matrix, thereby increasing the creep resistance of the alloy [30].

Other rare-earth elements have been investigated for the large lattice parameter of their  $\text{Al}_3\text{RE}$  ( $L1_2$ ) nanoprecipitates. In addition to Er, micro-additions (0.02 at.%) of Y, Sm, Gd, Tb, Dy, Ho, Tm, Yb or Lu, were investigated in Al-0.06Sc at.% [29–31]. Due to the faster diffusivity of the RE elements as compared to Sc, they are enriched in the core of the nanoprecipitates. The large lattice parameter mismatch of these core-shell  $\text{Al}_3(\text{Sc,RE})$  nanoprecipitates, created by the RE addition induces a drastic increase of creep strength at 300 °C. Based on microstructural characterization, microhardness, creep experiments and price, Er and Yb were identified as the most promising addition element to the  $L1_2$  strengthen Al–Sc alloys.

The simultaneous addition of Zr and Er to an Al–Sc alloy has the advantages of both ternary Al-based alloys [32]: (i) Er promotes early nucleation of a high number density of nanoprecipitates with an increased lattice parameter mismatch, which improves creep strength, and (ii) Zr slows the coarsening rate, thereby improving high-temperature stability of the nanoprecipitates. For example, a quaternary Al-0.05Sc-0.01Er-0.06Zr at.% alloy takes 30 min at 400 °C to achieve a microhardness plateau of  $\sim 450$  MPa, which is stable for at least 6 months at this temperature [32]. The nanoprecipitates display a complex core-double shell structure, with an Er-enriched core, a Sc-enriched inner shell and a Zr-rich outer shell. This core-double shell is a result of the differences in the diffusivities of the elements Er, Sc and Zr ( $D_{\text{Er}} > D_{\text{Sc}} > D_{\text{Zr}}$ ), which is why they precipitate sequentially.

The strength of the quaternary Al–Sc–Zr–Er alloy can further be increased by Si micro-additions [33–35]. Although Si does not form intermetallic compounds with Al, it forms M-Si-V clusters (M is a metal and V is a vacancy), which can diffuse faster than isolated M atoms in the  $\alpha$ -Al matrix, thus allowing faster growth and coarsening of the nanoprecipitates [36]. These clusters also serve as *nuclei* for heterogeneous precipitation and this increases the number density of nanoprecipitates and their volume fraction. For example, addition of 0.05 at.% Si to an Al-0.055Sc-0.005Er-0.02Zr at.% alloy increases the peak microhardness by 50 MPa, while reducing the aging heat treatment time from 1 h to 15 min [34]. Higher concentrations of Si further increase the alloy's strength [35]. Due to the enhanced solute diffusivity induced by silicon, the higher the Si concentration is, the faster the nanoprecipitates coarsen. Atom-probe tomography (APT) [37, 38] experiments demonstrate that Si additions also modify the concentration profiles associated with the nanoprecipitates. The nanoprecipitates exhibit a Sc/Er/Si enriched core, Si being located on the Al-sublattice, surrounded by a Zr-enriched shell instead of the core-double shell observed in Si-free alloys [34, 35]. The mechanisms underlying this structure are presently unclear, although it has been proposed to be due to either co-precipitation of  $(\text{Al,Si})_3(\text{Sc,Er})$  or due to the homogenization of the core-shell-structure during aging.

We investigated the use of In, Sb, Sr, Ge and Zn as a way to increase the number density of nanoprecipitates [39]. As for Si, these inoculants partition to the  $L1_2$  nanoprecipitates, as evidenced by LEAP tomographic analyses. These elements were usually found in the shell of the nanoprecipitates, alongside Zr. Antimony, however, stands out from the other elements due to an improvement of strength after long aging times. Because Si is a common impurity in commercially-pure aluminum, its use as an inoculant is the most convenient.

Attempts have been made to produce Sc-free Al–Er–Zr [40, 41] and Al–Er–Zr–Si [42] alloys by increasing strongly the Er concentration (0.04 at.%) and the Zr concentration to 0.1 at.%. As shown by Wen et al. [40, 41], additions of Zr to Al–Er alloys reduce the coarsening rate of the  $\text{Al}_3\text{Er}$  nanoprecipitates due to the formation of a Zr-enriched shell. The Al-0.04Er-0.08Zr alloy achieves a peak microhardness of 540 MPa after 64 h of aging at 400 °C. Due, however, to the sluggish diffusion of Zr in the aluminum matrix, the  $\text{Al}_3\text{Er}$  nanoprecipitates experience early coarsening behavior before the Zr-shell forms. There are no isothermal aging data on Al–Er–Zr alloys with Si additions; it is, however, expected that Si will accelerate the precipitation kinetics and causes stronger strengthening as detected for Al–Yb–Zr–Si alloys [43].

Although Sc-free Al–Er–Zr alloys are strong and inexpensive, the long aging times necessary to achieve peak

microhardness is a major drawback. With the accumulated knowledge from the past approximately 15 years of research on  $L_{12}$  forming elements and inoculants, rather than eliminating Sc from the Al–Sc–Er–Zr–Si alloys we maintained the Sc concentration of the alloy as small as possible, to minimize the alloy's cost [44, 45], but sufficiently high to prevent early coarsening of  $Al_3Er$  nanoprecipitates, by either forming a Sc-enriched shell or by co-precipitating with Er, thereby forming  $Al_3(Sc,Er)$  ( $L_{12}$ ) nanoprecipitates. We then compensated for the low Sc concentration by increasing the Zr concentration, while maintaining the Si concentration required to accelerate Zr precipitation. As compared to the previous Al-0.055Sc-0.005Er-0.02Zr-0.XY Si (at.%) alloys [34, 35], the majority of the expensive Sc has been replaced by the much less costly Zr, thereby reducing the Sc concentration by a factor 4 (from 0.055 to 0.015 at.%), and increasing concomitantly the Zr concentration by the same factor (from 0.02 to 0.08 at.%). To avoid the rapid coarsening of nanoprecipitates, due to the high Si concentration used previously [35], a relatively small Si concentration of 0.10 at.% was utilized. The very small Er concentration (0.005 at.%) remains unchanged. This low-Sc, high-Zr Al-0.08Zr-0.014Sc-0.008Er-0.10Si alloy achieved successfully a similar microhardness ( $\sim 575$  MPa) as the previous Sc-rich alloy, while demonstrating good coarsening resistance at high temperatures at a lower price (estimated at  $\sim 6$  USD/kg vs.  $\sim 16$  USD/kg [46, 47]). LEAP tomographic analyses revealed the formation of a nearly stoichiometric  $Al_3Zr$  shell enveloping a Sc- and Er-enriched core (Fig. 1), highlighting the strong confining effect of Zr on these two elements [44, 45]. The creep resistance of this alloy at 300 °C is comparable to an Al-0.08Sc binary alloy. Zirconium being the main alloying element, annealing for 24 h is necessary to achieve a peak microhardness, which is a

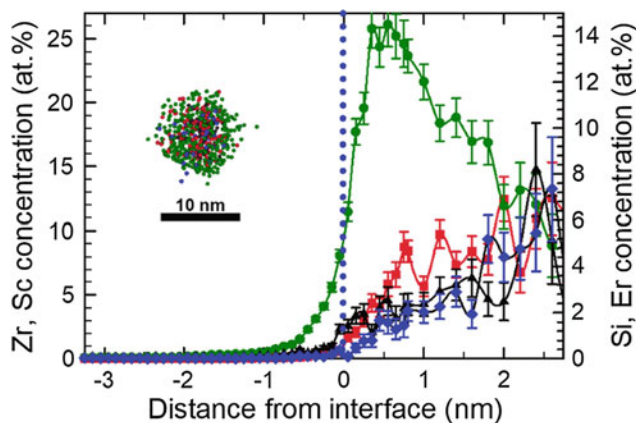


**Fig. 1** Typical nanoprecipitate observed by LEAP tomography in a Al-0.08Zr-0.014Sc-0.008Er-0.10Si alloy [44, 45] and its associated proximity histogram [48]. The Zr enriched shell envelops the Er-, Sc- and Si- enriched core, improving the coarsening resistance at high temperature

significant improvement when compared to the hundreds of hours needed for the Sc-free alloys, highlighting the need to maintain Sc at smaller concentrations.

In an attempt to increase the maximum operating temperature beyond 400 °C, a temperature beyond which the Zr diffusivity becomes too high and concomitantly coarsening too fast, we have investigated  $L_{12}$  forming elements, such as Ti, Hf, V, Nb and Ta, with diffusivities smaller than that of Zr [49–51]. The addition of Ti to Al–Zr revealed itself unfruitful. Although Ti was found to partition into the  $Al_3(Zr,Ti)$  nanoprecipitates [52], it had no effects on their growth and coarsening kinetic, or preventing its transformation from the  $L_{12}$  to the  $DO_{23}$  structure at long aging duration [18, 19], while having negative impact on creep resistance [53]. The addition of 0.08 at.% Hf to an Al-0.11Zr-0.045Er alloy created a number of challenges [51]. Due to the strong peritectic segregation of Hf in the dendritic structure, alongside Zr, homogenization annealing lead to a loss of solute, which prevented strengthening. A strong positive effect was observed with the simultaneous addition of small concentrations of Si and Fe. As indicated, Si is known to increase the precipitation kinetics and improve peak microhardness. Iron, however, is an undesirable impurity that scavenges RE elements in aluminum alloys [54]. This unexpected positive effect of Fe (when present with Si) on strengthening opens the door to the use of commercial-purity aluminum, whose two main impurities are Fe and Si. The alloy reached a microhardness of  $\sim 500$  MPa after 24 h of aging at 400 °C, which was maintained for 2,000 h. As anticipated, LEAP tomographic analyses revealed a Hf-enriched shell around the  $Al_3(Zr,Er,Hf)$  nanoprecipitates.

The addition of 0.08 at.% V to an Al-0.07Zr-0.02Sc-0.005Er-0.06Si [49] lead to slightly improved microhardness values and a coarsening resistance when aged at 400 and 425 °C, when compared to the V-free alloy, consistent with a LEAP analysis showing slight partitioning of V to the shell of the  $Al_3(Zr,Sc,Er,V)$  nanoprecipitates. This segregation of V to the matrix/precipitate interface reduces the lattice parameter misfit, which increases the coarsening resistance of the nanoprecipitates. Although  $Al_3V$  exhibit a negative lattice mismatch with the matrix, as opposed to a positive lattice mismatch for  $Al_3Sc$ ,  $Al_3Er$  and  $Al_3Zr$ , the creep strength of the alloy was not reduced, and was, in fact, comparable to the V-free alloy. Additions of 0.05 at.% of Nb or Ta was also investigated [50], and similarly to V, these transition elements also partition to the  $L_{12}$  matrix/precipitate interface, at concentration levels of 1% and 0.5%, respectively. Both Nb- and Ta-modified alloys exhibited higher peak microhardness values after a double-aging heat-treatment ( $\sim 575$  and  $\sim 600$  MPa) and improved coarsening resistance at 400 °C, when compared to the V modified alloy.

Over the last two decades of research at Northwestern University, each new generation of  $L1_2$ -strengthened aluminum alloy has further pushed the upper use temperature in terms of coarsening and creep resistance, which are both intimately linked with maintaining nano-size, coherent  $L1_2$ -structured nanoprecipitates. Starting with a maximum temperature of 300 °C for the extremely expensive binary Al-Sc and ternary Al-Mg-Sc alloys, we have progressively increased the complexity of the alloy by controlled micro-additions of transition metals (for coarsening resistance), lanthanoids (for nucleation improvement and creep resistance) and metalloids (for nucleation and diffusivity improvements), while also considering solid-solution strengthening, with Mg [55, 56] or Li [57, 58], secondary nanoprecipitates (e.g., metastable coherent  $Al_3Li$  ( $L1_2$ ) nanoprecipitates [59]), and oxide dispersoids [60]. Our most recent aluminum superalloys can withstand temperatures in the 400–425 °C range due to the improved coarsening resistance of the alloy with similar or improved mechanical properties and with the additional benefit of a significant reduction in the cost of the alloy.

**Acknowledgements** The authors acknowledge partial support from the Ford-Northwestern University Alliance. DNS and DCD also acknowledge the support of the Office of Naval Research (N00014-16-1-2402). DNS and DCD disclose that they have a financial interest in NanoAl LLC which is active in the area of aluminum alloys. The authors kindly thank Drs. J. Boileau and B. Ghaffari (Ford Research Laboratory) for numerous useful discussions.

## References

1. P.K. Mallick, *Materials, design and manufacturing for lightweight vehicles*, CRC Press; Woodhead, Boca Raton, Fla.: Oxford, 2010.
2. K.E. Knipling, D.C. Dunand, D.N. Seidman, Criteria for developing castable, creep-resistant aluminum-based alloys – A review, *Z. Für Met.* 97 (2006) 246–265. doi:<https://doi.org/10.3139/146.101249>.
3. T. Torma, E. Kovács-Csetényi, T. Turmezey, T. Ungár, I. Kovács, Hardening mechanisms in Al-Sc alloys, *J Mater Sci.* 24 (1989) 3924–3927. doi:<https://doi.org/10.1007/BF01168955>.
4. H.-H. Jo, S.-I. Fujikawa, Kinetics of precipitation in Al3Sc alloys and low temperature solid solubility of scandium in aluminium studied by electrical resistivity measurements, *Materials Science and Engineering: A.* 171 (1993) 151–161. doi:[https://doi.org/10.1016/0921-5093\(93\)90401-Y](https://doi.org/10.1016/0921-5093(93)90401-Y).
5. L.S. Toropova, D.G. Eskin, M.L. Kharakterova, T.V. Dobatkina, eds., *Advanced aluminum alloys containing scandium: structure and properties*, Gordon & Breach, Amsterdam, 1998.
6. V.G. Davydov, T.D. Rostova, V.V. Zakharov, Y.A. Filatov, V.I. Yelagin, Scientific principles of making an alloying addition of scandium to aluminium alloys, *Materials Science and Engineering: A.* 280 (2000) 30–36. doi:[https://doi.org/10.1016/S0921-5093\(99\)00652-8](https://doi.org/10.1016/S0921-5093(99)00652-8).
7. V.V. Zakharov, Effect of Scandium on the Structure and Properties of Aluminum Alloys, *Metal Science and Heat Treatment.* 45 (2003) 246–253. doi:<https://doi.org/10.1023/A:1027368032062>.
8. N.A. Belov, A.N. Alabin, D.G. Eskin, V.V. Istomin-Kastrovskii, Optimization of hardening of Al-Zr-Sc cast alloys, *J Mater Sci.* 41 (2006) 5890–5899. doi:<https://doi.org/10.1007/s10853-006-0265-7>.
9. A. Deschamps, L. Lae, P. Guyot, In situ small-angle scattering study of the precipitation kinetics in an Al-Zr-Sc alloy, *Acta Materialia.* 55 (2007) 2775–2783. doi:<https://doi.org/10.1016/j.actamat.2006.12.015>.
10. J. Royset, Scandium In Aluminium Alloys: Physical Metallurgy, Properties And Applications, *Metallurgical Science and Technology.* 25 (2013).
11. S. Riva, K.V. Yusenko, N.P. Lavery, D.J. Jarvis, S.G.R. Brown, The scandium effect in multicomponent alloys, *International Materials Reviews.* 61 (2016) 203–228. doi:<https://doi.org/10.1080/09506608.2015.1137692>.
12. C. Yang, P. Zhang, D. Shao, R.H. Wang, L.F. Cao, J.Y. Zhang, G. Liu, B.A. Chen, J. Sun, The influence of Sc solute partitioning on the microalloying effect and mechanical properties of Al-Cu alloys with minor Sc addition, *Acta Materialia.* 119 (2016) 68–79. doi:<https://doi.org/10.1016/j.actamat.2016.08.013>.
13. H. Bo, L.B. Liu, J.L. Hu, Z.P. Jin, Experimental study and thermodynamic modeling of the Al-Sc-Zr system, *Computational Materials Science.* 133 (2017) 82–92. doi:<https://doi.org/10.1016/j.commatsci.2017.02.029>.
14. E.A. Marquis, D.N. Seidman, Nanoscale structural evolution of Al3Sc precipitates in Al(Sc) alloys, *Acta Materialia.* 49 (2001) 1909–1919. doi:[https://doi.org/10.1016/S1359-6454\(01\)00116-1](https://doi.org/10.1016/S1359-6454(01)00116-1).
15. D.N. Seidman, E.A. Marquis, D.C. Dunand, Precipitation strengthening at ambient and elevated temperatures of heat-treatable Al (Sc) alloys, *Acta Materialia.* 50 (2002) 4021–4035. doi:[https://doi.org/10.1016/S1359-6454\(02\)00201-X](https://doi.org/10.1016/S1359-6454(02)00201-X).
16. E. Nes, Precipitation of the metastable cubic Al3Zr-phase in superinterstitial Al-Zr alloys, *Acta Metallurgica.* 20 (1972) 499–506. doi:[https://doi.org/10.1016/0001-6160\(72\)90005-3](https://doi.org/10.1016/0001-6160(72)90005-3).
17. K.E. Knipling, D.C. Dunand, D.N. Seidman, Nucleation and Precipitation Strengthening in Dilute Al-Ti and Al-Zr Alloys, *Metallurgical and Materials Transactions A.* 38 (2007) 2552–2563. doi:<https://doi.org/10.1007/s11661-007-9283-6>.
18. K.E. Knipling, D.C. Dunand, D.N. Seidman, Precipitation evolution in Al-Zr and Al-Zr-Ti alloys during isothermal aging at 375–425 °C, *Acta Materialia.* 56 (2008) 114–127. doi:<https://doi.org/10.1016/j.actamat.2007.09.004>.
19. K.E. Knipling, D.C. Dunand, D.N. Seidman, Precipitation evolution in Al-Zr and Al-Zr-Ti alloys during aging at 450–600 °C, *Acta Materialia.* 56 (2008) 1182–1195. doi:<https://doi.org/10.1016/j.actamat.2007.11.011>.
20. H. Li, J. Bin, J. Liu, Z. Gao, X. Lu, Precipitation evolution and coarsening resistance at 400 °C of Al microalloyed with Zr and Er, *Scripta Materialia.* 67 (2012) 73–76. doi:<https://doi.org/10.1016/j.scriptamat.2012.03.026>.
21. E. Çadirli, H. Tecer, M. Şahin, E. Yılmaz, T. Kirindi, M. Gündüz, Effect of heat treatments on the microhardness and tensile strength of Al-0.25wt.% Zr alloy, *Journal of Alloys and Compounds.* 632 (2015) 229–237. doi:<https://doi.org/10.1016/j.jallcom.2015.01.193>.
22. M.E. van Dalen, R.A. Karnesky, J.R. Cabotaje, D.C. Dunand, D. N. Seidman, Erbium and ytterbium solubilities and diffusivities in aluminum as determined by nanoscale characterization of precipitates, *Acta Materialia.* 57 (2009) 4081–4089. doi:<https://doi.org/10.1016/j.actamat.2009.05.007>.
23. Y. Zhang, K. Gao, S. Wen, H. Huang, Z. Nie, D. Zhou, The study on the coarsening process and precipitation strengthening of Al3Er precipitate in Al-Er binary alloy, *Journal of Alloys and Compounds.* 610 (2014) 27–34. doi:<https://doi.org/10.1016/j.jallcom.2014.04.093>.

24. C.B. Fuller, D.N. Seidman, D.C. Dunand, Mechanical properties of Al(Sc,Zr) alloys at ambient and elevated temperatures, *Acta Materialia*. 51 (2003) 4803–4814. doi:[https://doi.org/10.1016/S1359-6454\(03\)00320-3](https://doi.org/10.1016/S1359-6454(03)00320-3).
25. C. Fuller, J. Murray, D. Seidman, Temporal evolution of the nanostructure of Al(Sc,Zr) alloys: Part I – Chemical compositions of Al(Sc,Zr) precipitates, *Acta Materialia*. 53 (2005) 5401–5413. doi:<https://doi.org/10.1016/j.actamat.2005.08.016>.
26. C. Fuller, D. Seidman, Temporal evolution of the nanostructure of Al(Sc,Zr) alloys: Part II-coarsening of Al(Sc,Zr) precipitates, *Acta Materialia*. 53 (2005) 5415–5428. doi:<https://doi.org/10.1016/j.actamat.2005.08.015>.
27. K.E. Knipling, R.A. Karnesky, C.P. Lee, D.C. Dunand, D.N. Seidman, Precipitation evolution in Al–0.1Sc, Al–0.1Zr and Al–0.1Sc–0.1Zr (at.%) alloys during isochronal aging, *Acta Materialia*. 58 (2010) 5184–5195. doi:<https://doi.org/10.1016/j.actamat.2010.05.054>.
28. K.E. Knipling, D.N. Seidman, D.C. Dunand, Ambient- and high-temperature mechanical properties of isochronally aged Al–0.06Sc, Al–0.06Zr and Al–0.06Sc–0.06Zr (at.%) alloys, *Acta Materialia*. 59 (2011) 943–954. doi:<https://doi.org/10.1016/j.actamat.2010.10.017>.
29. R.A. Karnesky, M.E. van Dalen, D.C. Dunand, D.N. Seidman, Effects of substituting rare-earth elements for scandium in a precipitation-strengthened Al–0.08at. %Sc alloy, *Scripta Materialia*. 55 (2006) 437–440. doi:<https://doi.org/10.1016/j.scriptamat.2006.05.021>.
30. R.A. Karnesky, D.N. Seidman, D.C. Dunand, Creep of Al-Sc Microalloys with Rare-Earth Element Additions, *Materials Science Forum*. 519–521 (2006) 1035–1040. doi:<https://doi.org/10.4028/www.scientific.net/MSF.519-521.1035>.
31. M.E. Krug, A. Werber, D.C. Dunand, D.N. Seidman, Core-shell nanoscale precipitates in Al–0.06 at. % Sc microalloyed with Tb, Ho, Tm or Lu, *Acta Materialia*. 58 (2010) 134–145. doi:<https://doi.org/10.1016/j.actamat.2009.08.074>.
32. C. Booth-Morrison, D.C. Dunand, D.N. Seidman, Coarsening resistance at 400 °C of precipitation-strengthened Al–Zr–Sc–Er alloys, *Acta Mat.* 59 (2011) 7029–7042. doi:<https://doi.org/10.1016/j.actamat.2011.07.057>.
33. C. Booth-Morrison, D.N. Seidman, D.C. Dunand, Effect of Er additions on ambient and high-temperature strength of precipitation-strengthened Al–Zr–Sc–Si alloys, *Acta. Mat.* 60 (2012) 3643–3654. doi:<https://doi.org/10.1016/j.actamat.2012.02.030>.
34. N.Q. Vo, D.C. Dunand, D.N. Seidman, Improving aging and creep resistance in a dilute Al–Sc alloy by microalloying with Si, Zr and Er, *Acta. Mat.* 63 (2014) 73–85. doi:<https://doi.org/10.1016/j.actamat.2013.10.008>.
35. N.Q. Vo, D.C. Dunand, D.N. Seidman, Role of silicon in the precipitation kinetics of dilute Al-Sc-Er-Zr alloys, *Materials Science and Engineering: A*. 677 (2016) 485–495. doi:<https://doi.org/10.1016/j.msea.2016.09.065>.
36. C. Booth-Morrison, Z. Mao, M. Diaz, D.C. Dunand, C. Wolverton, D.N. Seidman, Role of silicon in accelerating the nucleation of Al<sub>3</sub>(Sc,Zr) precipitates in dilute Al–Sc–Zr alloys, *Acta. Mat.* 60 (2012) 4740–4752. doi:<https://doi.org/10.1016/j.actamat.2012.05.036>.
37. D.N. Seidman, Three-Dimensional Atom-Probe Tomography: Advances and Applications, *Annual Review of Materials Research*. 37 (2007) 127–158. doi:<https://doi.org/10.1146/annurev.matsci.37.052506.084200>.
38. D.N. Seidman, K. Stiller, An Atom-Probe Tomography Primer, *MRS Bulletin*. 34 (2009) 717–724. doi:<https://doi.org/10.1557/mrs2009.194>.
39. J.D. Lin, P. Okle, D.C. Dunand, D.N. Seidman, Effects of Sb micro-alloying on precipitate evolution and mechanical properties of a dilute Al-Sc-Zr alloy, *Materials Science and Engineering: A*. 680 (2017) 64–74. doi:<https://doi.org/10.1016/j.msea.2016.10.067>.
40. S.P. Wen, K.Y. Gao, Y. Li, H. Huang, Z.R. Nie, Synergetic effect of Er and Zr on the precipitation hardening of Al–Er–Zr alloy, *Scripta Materialia*. 65 (2011) 592–595. doi:<https://doi.org/10.1016/j.scriptamat.2011.06.033>.
41. S.P. Wen, K.Y. Gao, H. Huang, W. Wang, Z.R. Nie, Precipitation evolution in Al–Er–Zr alloys during aging at elevated temperature, *Journal of Alloys and Compounds*. 574 (2013) 92–97. doi:<https://doi.org/10.1016/j.jallcom.2013.03.237>.
42. N.Q. Vo, D.N. Seidman, D.C. Dunand, Aluminum superalloys for use in high temperature applications, US20150259773, 2015.
43. S.P. Wen, K.Y. Gao, H. Huang, W. Wang, Z.R. Nie, Role of Yb and Si on the precipitation hardening and recrystallization of dilute Al–Zr alloys, *Journal of Alloys and Compounds*. 599 (2014) 65–70. doi:<https://doi.org/10.1016/j.jallcom.2014.02.065>.
44. A. De Luca, D.C. Dunand, D.N. Seidman, Mechanical properties and optimization of the aging of a dilute Al-Sc-Er-Zr-Si alloy with a high Zr/Sc ratio, *Acta Materialia*. 119 (2016) 35–42. doi:<https://doi.org/10.1016/j.actamat.2016.08.018>.
45. A. De Luca, D.C. Dunand, D.N. Seidman, Microstructure and mechanical properties of a precipitation-strengthened Al-Zr-Sc-Er-Si alloy with a very small Sc content, *Acta Materialia*. 144(2018) 80–91. doi:<https://doi.org/10.1016/j.actamat.2017.10.040>.
46. Mineralprices.com, (n.d.). <http://mineralprices.com/> (accessed October 12, 2017).
47. U.S. Geological Survey, Metal prices in the United States through 2010: U.S. Geological Survey Scientific Investigations Report 2012–5188, 204 p, (2013).
48. O.C. Hellman, J.A. Vandembroucke, J. Rüsing, D. Isheim, D.N. Seidman, Analysis of Three-dimensional Atom-probe Data by the Proximity Histogram, *Microsc. Microanal.* 6 (2000) 437–444.
49. D. Erdeniz, W. Nasim, J. Malik, A.R. Yost, S. Park, A. De Luca, N. Q. Vo, I. Karaman, B. Mansoor, D.N. Seidman, D.C. Dunand, Effect of vanadium micro-alloying on the microstructural evolution and creep behavior of Al-Er-Sc-Zr-Si alloys, *Acta Materialia*. 124 (2017) 501–512. doi:<https://doi.org/10.1016/j.actamat.2016.11.033>.
50. D. Erdeniz, A. De Luca, D.N. Seidman, D.C. Dunand, Effect of Nb and Ta Additions on Strength and Coarsening Resistance of Precipitation-Strengthened Al-Zr-Sc-Er-Si Alloys, Unpublished.
51. R.A. Michi, D.C. Dunand, D.N. Seidman, Effects of Si and Fe Micro-additions on the Aging Response of a Dilute Al-0.045Er-0.08Hf-0.08Zr (at.%) Alloy, Unpublished.
52. K.E. Knipling, D.C. Dunand, D.N. Seidman, Atom Probe Tomographic Studies of Precipitation in Al-0.1Zr-0.1Ti (at.%) Alloys, *Microscopy and Microanalysis*. 13 (2007) 503–516. doi:<https://doi.org/10.1017/S1431927607070882>.
53. K.E. Knipling, D.C. Dunand, Creep resistance of cast and aged Al–0.1Zr and Al–0.1Zr–0.1Ti (at.%) alloys at 300–400 °C, *Scripta Materialia*. 59 (2008) 387–390. doi:<https://doi.org/10.1016/j.scriptamat.2008.02.059>.
54. O. Beerli, D.C. Dunand, D.N. Seidman, Roles of impurities on precipitation kinetics of dilute Al–Sc alloys, *Mat. Sci. Eng. A*. 527 (2010) 3501–3509. doi:<https://doi.org/10.1016/j.msea.2010.02.027>.
55. E.A. Marquis, D.N. Seidman, D.C. Dunand, Effect of Mg addition on the creep and yield behavior of an Al–Sc alloy, *Acta Materialia*. 51 (2003) 4751–4760. doi:[https://doi.org/10.1016/S1359-6454\(03\)00288-X](https://doi.org/10.1016/S1359-6454(03)00288-X).
56. E.A. Marquis, D.N. Seidman, Coarsening kinetics of nanoscale Al<sub>3</sub>Sc precipitates in an Al–Mg–Sc alloy, *Acta Materialia*.

- 53 (2005) 4259–4268. doi:<https://doi.org/10.1016/j.actamat.2005.05.025>.
57. M.E. Krug, D.C. Dunand, D.N. Seidman, Effects of Li additions on precipitation-strengthened Al–Sc and Al–Sc–Yb alloys, *Acta Materialia*. 59 (2011) 1700–1715. doi:<https://doi.org/10.1016/j.actamat.2010.11.037>.
58. M.E. Krug, D.N. Seidman, D.C. Dunand, Creep properties and precipitate evolution in Al–Li alloys microalloyed with Sc and Yb, *Materials Science and Engineering: A*. 550 (2012) 300–311. doi:<https://doi.org/10.1016/j.msea.2012.04.075>.
59. M.E. Krug, D.C. Dunand, D.N. Seidman, Composition profiles within Al<sub>3</sub>Li and Al<sub>3</sub>Sc/Al<sub>3</sub>Li nanoscale precipitates in aluminum, *Appl. Phys. Lett.* 92 (2008) 124107. doi:<https://doi.org/10.1063/1.2901150>.
60. R.A. Karnesky, L. Meng, D.C. Dunand, Strengthening mechanisms in aluminum containing coherent Al<sub>3</sub>Sc precipitates and incoherent Al<sub>2</sub>O<sub>3</sub> dispersoids, *Acta Materialia*. 55 (2007) 1299–1308. doi:<https://doi.org/10.1016/j.actamat.2006.10.004>.